BIOCHEMISTRY
including biophysical chemistry & molecular biology

Article

pubs.acs.org/biochemistry

Bilberry Anthocyanins Neutralize the Cytotoxicity of Co-Chaperonin GroES Fibrillation Intermediates

Hisanori Iwasa,[†,#] Hiroshi Kameda,[†,#] Naoya Fukui,[†] Sakiho Yoshida,[‡] Kunihiro Hongo,[†,‡] Tomohiro Mizobata,[†,‡] Saori Kobayashi,[§] and Yasushi Kawata*[,†,‡]

[†]Department of Chemistry and Biotechnology, Graduate School of Engineering, [‡]Department of Biomedical Science, Institute of Regenerative Medicine and Biofunction, Graduate School of Medical Science, Tottori University, Tottori 680-8552, Japan

[§]Wakasa Seikatsu Co., Ltd., Research Park 1st Building, 134 Chudoujiminami-cho, Shimogyo-ku, Kyoto 600-8813, Japan

ABSTRACT: The co-chaperonin GroES (Hsp10) works with chaperonin GroEL (Hsp60) to facilitate the folding reactions of various substrate proteins. Upon forming a specific disordered state in guanidine hydrochloride, GroES is able to self-assemble into amyloid fibrils similar to those observed in various neurodegenerative diseases. GroES therefore is a suitable model system to understand the mechanism of amyloid fibril formation. Here, we determined the cytotoxicity of intermediate GroES species formed during fibrillation. We found that neuronal cell death was provoked by soluble intermediate aggregates of GroES, rather than mature fibrils. The data suggest that amyloid fibril formation and its associated toxicity toward cell might be an inherent property of proteins irrespective of their correlation with specific diseases. Furthermore, with the presence of anthocyanins that are abundant in bilberry, we could inhibit both fibril formation and the toxicity of intermediates. Addition of bilberry anthocyanins dissolved the toxic intermediates and fibrils, and the toxicity of the intermediates was thus neutralized. Our results suggest that anthocyanins may display a general and potent inhibitory effect on the amyloid fibril formation of various conformational disease-causing proteins.

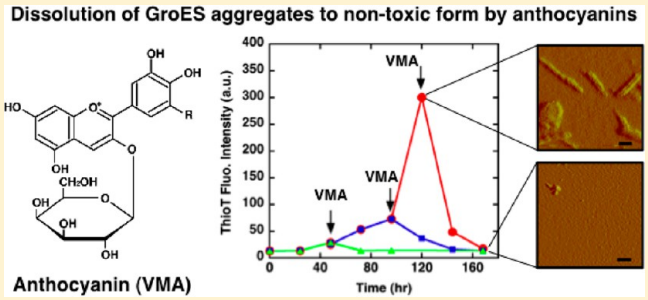

Amyloid fibrils are insoluble aggregated forms of proteins with ordered structure, commonly observed as deposits in tissues of patients with various amyloidoses.[1−3] Among the proteins correlated with various neurological disorders diseases to date, several proteins, including Aβ (Alzheimer's disease), α-synuclein (Parkinson's disease), and huntingtin (Huntington's disease),[4,5] have been found to be intrinsically disordered proteins that do not adopt a well-defined structure in a free state.[6] Intrinsically disordered proteins are abundant in eukaryotic proteins and play a number of biologically significant roles, by folding into highly ordered conformations upon binding to their cellular targets.[7] Although it was previously assumed that the pathological mechanisms of diseases correlated to intrinsically disordered proteins involved the mature amyloid fibril form of these proteins, recent studies have indicated that the toxicity is derived from initial soluble oligomeric forms that are formed before the insoluble, fully formed fibrils.[8,9] Further, there is increasing evidence that amyloid fibrils closely similar to those associated with clinical amyloidoses may also be formed *in vitro* from various proteins unrelated to disease, and this suggests that a general mechanism involving proteins/polypeptide fibrillation and toxicity may be attainable.[10,11]

Currently, many treatments of amyloid-related degenerative diseases are palliative, and therapeutic agents that are directed toward preventing or abolishing the underlying process of protein fibril formation have yet to be found. One important approach in this latter effort is the use of small molecular compounds that specifically and efficiently inhibit fibril formation.[12] Although several types of small molecular compounds and small polyphenols have been found to act as inhibitory agents for *in vitro* protein fibrillation and associated cytotoxicity,[12,13] accumulating fundamental knowledge on these compounds and their action remains important.

The co-chaperonin GroES, a member of the 10 kDa heat shock proteins from *Escherichia coli*, plays a significant role in protein folding by working with the chaperonin GroEL to suppress aggregation and facilitate the folding of various substrate proteins *in vivo* and *in vitro*.[14,15] GroES adopts a unique dome-like structure composed of seven identical subunits (10 kDa) rich in β-strands.[16,17] A number of studies regarding the structural stability, unfolding, and refolding of GroES have been performed.[18−22] In the course of such studies, we previously found that when GroES samples were incubated for an extended interval in solutions containing guanidine hydrochloride (Gdn-HCl), the samples formed highly viscous gels, which displayed characteristics common to amyloid fibrils.[23] We subsequently determined that this fibrillation of

Received: August 19, 2013
Revised: November 13, 2013
Published: December 6, 2013

   dx.doi.org/10.1021/bi401135j | *Biochemistry* 2013, 52, 9202−9211

GroES was a good model to use in understanding the general mechanism of protein fibrillation. In addition, since fibrils of GroES were formed from samples unfolded extensively in Gdn-HCl,[24,25] the system may provide interesting details on the fibril formation of proteins that are highly disordered or intrinsically unfolded in the cell.

Here, we set out to investigate whether GroES amyloid fibrils or associated molecular intermediates could display cytotoxicity, by adding various species derived from the reaction to neuronal cell cultures. We also tested the inhibitory effects of small polyphenols obtained from extracts of bilberry (*Vaccinium myrtillus* anthocyanoside, VMA). Bilberries are an abundant source of natural polyphenols with structures similar to the polyphenol inhibitors previously reported in various studies involving *in vitro* amyloid fibril formation of intrinsically disordered proteins.[12,13] Interestingly, we found that intermediate species of GroES formed during fibrillation display toxicity toward cell cultures, and both this cytotoxicity and formation of fibrils were inhibited by addition of bilberry anthocyanins. Surprisingly, we found that adding the polyphenols resulted in the resolubiliation of GroES amyloid fibrils and toxic intermediate molecular species. The findings obtained from our experiments provide insights into the general mechanism of amyloid fibril formation and the toxicity of intermediate aggregate forms, as well as demonstrate that bilberry polyphenols act as potent inhibitors of fibril formation and toxicity.

MATERIALS AND METHODS

Preparation of GroES. GroES protein was expressed in *E. coli* BL21(DE3) (Novagen) and purified as described previously.[20,25] Purified GroES samples were dialyzed against Milli-Q water and stocked at 4 °C after lyophilization. The purity of GroES was checked by SDS-PAGE. The concentration of GroES protein was determined by using either an extinction coefficient determined at 280 nm (1 mg/mL of absorbance in path length of 1 cm is 0.143 (ref 26)) or a protein dye assay (protein assay kit, Bio-Rad Laboratories) using bovine serum albumin (Sigma) as a standard.

Amyloid Fibril Formation and ThioT Binding Assay. Experiments of amyloid fibril formation were performed with 1 mg/mL (96 μM monomer) GroES dissolved in 50 mM sodium phosphate buffer (pH 7.4) containing 1.6 M Gdn-HCl with linear agitation at 37 °C in glass test tubes. ThioT fluorescence was measured using a F-4500 fluorescence spectrophotometer (Hitachi) at 25 °C. At appropriate times, aliquots of GroES samples were withdrawn and mixed thoroughly with staining solution (25 μM ThioT, 5 mM sodium phosphate (pH 7.4), 150 mM NaCl). The concentration of GroES during measurement was 7.5 μg/mL. Fluorescence intensities were monitored at 480 nm with excitation at 440 nm. VMA was provided by Wakasa Seikatsu Co. Ltd. (Kyoto), and the purified polyphenols delphinidin, cyanidin, delphinidin 3-galactoside (del 3-gal), and cyanidin 3-galactoside (cya 3-gal) were purchased from Tokiwa Phytochemical.

Preparation of Soluble Aggregates, Amyloid Fibrils, and Amorphous Species for Cytotoxicity Assays. Aliquots of GroES samples incubated in Gdn-HCl for the appropriate times were ultracentrifuged for 1 h at 174000*g* and 4 °C. Supernatant fractions were subjected to a desalting PD Spin Trap G-25 (GE Healthcare) in order to remove Gdn-HCl. Mature amyloid fibrils isolated in precipitates after ultracentrifugation were suspended in 50 mM sodium phosphate buffer (pH 7.4), ultracentrifuged, then resuspended in the same buffer. Sonicated fibrils were prepared by ultracentrifugation of mature fibril samples (determined by Thio-T assay) and resuspending the pellets in 50 mM sodium phosphate buffer (pH 7.4). These samples were sonicated for 30 s using a Vibracell sonicator (Sonics and Materials). For preparation of amorphous aggregated species, native GroES was dissolved in 50 mM sodium phosphate (pH 7.4) containing 0.5 M Gdn-HCl (a denaturant concentration where GroES is partially unfolded[19,24]) and diluted 10-fold with 20 mM Glycine-HCl (pH 3.4). After 24 h, samples were centrifuged (18000*g*, 10 min, 4 °C), and the supernatant and amorphous precipitates were collected.

MTS Assay. Mouse neuroblastoma Neuro-2a cells (ECACC) were plated onto 48-well plates and cultured in a humidified chamber containing 5% (v/v) CO_2 at 37 °C in MEM medium supplemented with 10% (v/v) heat-inactivated fetal bovine serum, 0.1 mM MEM nonessential amino acids, 1 mM sodium pyruvate, 100 U/mL penicillin, and 100 μg/mL streptomycin. These reagents were purchased from GIBCO. When cells reached confluence (~50 000 cells per well), the medium was replaced with serum-free medium. Cells were then exposed to 10 μg of GroES samples for 24 h. Cell viability was assessed using the AQueous one solution cell proliferation assay (Promega) following the manufacturer's instructions. The absorbance at 490 nm was recorded for MTS reduction using an Infinite M200 (TECAN) or SpectraMax M2^e (Molecular Devices) plate reader. The percentage of cell viability was normalized as follows: 0% corresponds to the absorbance value obtained when cells were treated with 10 μM melittin from honey bee venom (Sigma), and 100% corresponds to the absorbance value obtained when cells were treated with 50 mM sodium phosphate buffer.

DiBAC$_4$(3) Assay. Changes in cell membrane potential were detected using a bisoxonol dye, bis-(1,3-dibutylbarbituric acid) trimethine oxonol (DiBAC$_4$(3), Dojindo), following the method provided by the manufacturer. Confluent Neuro-2a cells cultured in 48-well plates were rinsed twice with assay buffer (20 mM HEPES (pH 7.4), 120 mM NaCl, 2 mM KCl, 2 mM $CaCl_2$, 1 mM $MgCl_2$, 5 mM glucose, 5 μM DiBAC$_4$(3)) and incubated with assay buffer in a cell incubator for 30 min. Ten micrograms of GroES samples was added to each well and incubated for 5 min at 37 °C. Then, fluorescence intensities were measured at 37 °C using an Infinite M200 (TECAN) plate reader with excitation and emission wavelengths of 495 and 517 nm, respectively. The percentage of the relative fluorescence intensity of DiBAC$_4$(3) was normalized as follows: 0% corresponds to the fluorescence intensity detected from cells treated with 50 mM sodium phosphate buffer and 100% corresponds to the fluorescence intensity detected from cells treated with 10 μM melittin.

Transmission Electron Microscopy (TEM). TEM measurements were performed on a JEOL-100CX transmission electron microscope operated at 80 kV, as previously described.[27] Samples (1 mg/mL GroES protein) were diluted 10-fold with water and negatively stained with 2% (w/v) uranyl acetate solution on copper grids (400-mesh) covered by carbon-coated collodion film (Nisshin EM).

Atomic Force Microscopy (AFM). AFM measurements were performed on a Digital Instruments Nanoscope IV scanning microscope (model MMAFM-2) at 25 °C. Measurements were performed using tapping mode in air atmosphere. Fifteen microliters of 10-fold diluted fibril solution was put

dx.doi.org/10.1021/bi401135j | *Biochemistry* 2013, 52, 9202−9211

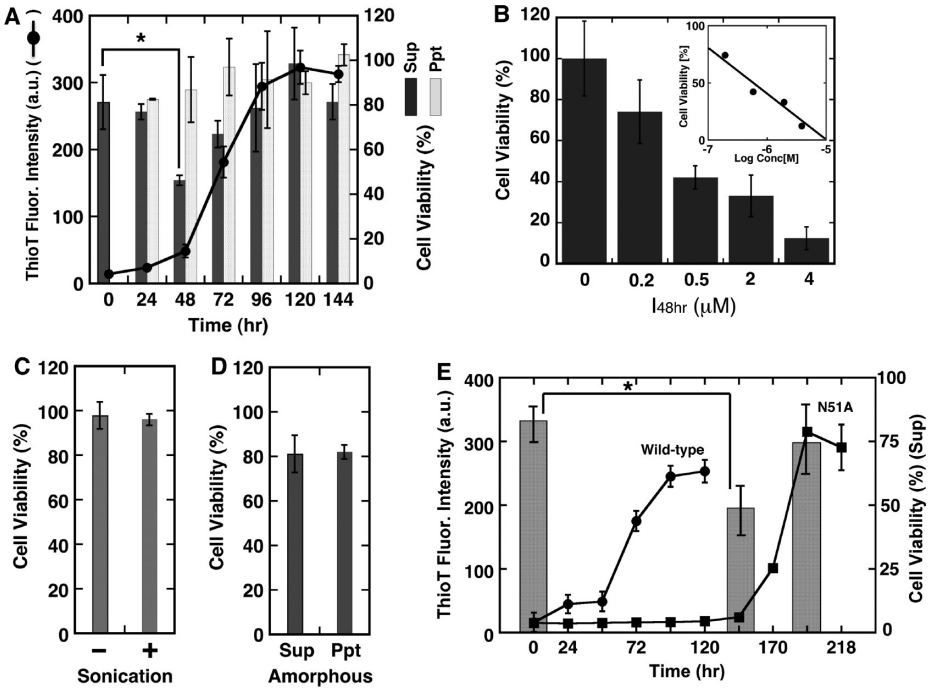

Figure 1. Cytotoxicity evaluation of GroES species formed during amyloid fibril formation and nonspecific aggregation. (A) Amyloid fibril formation of GroES traced by ThioT fluorescence and MTS assay. 96 μM GroES samples were incubated in 50 mM sodium phosphate buffer (pH 7.4) containing 1.6 M Gdn-HCl with linear agitation at 37 °C. At appropriate times, aliquots of samples were withdrawn and separated into Gdn-HCl-free supernatant and precipitate fractions as described in Materials and Methods, followed by sterile addition to Neuro-2a culture medium. Statistical significance was calculated by using Student's *t*-test: $*p < 0.05$. (B) Determination of IC50 of toxic intermediates formed after 48 h incubation (I48hr). The IC50 (0.6 μM) was estimated by plotting of dose-dependent cell viability (inset figure). (C and D) MTS cell viability assays upon addition of mature intact and sonicated fibrils (C) and of supernatant and precipitate fractions derived from nonspecific amorphous species of GroES (D). (E) Amyloid fibril formation of GroES N51A mutant traced by ThioT fluorescence (square symbols) and MTS assay (gray bars) ($*p < 0.05$). For comparison, the fibril formation trace of wild-type GroES monitored by ThioT fluorescence is also plotted (circle symbols). Experimental conditions were the same as in A.

onto freshly cleaved mica, incubated for 30 min, and then washed with 200 μL of water and dried.

RESULTS

Amyloid Fibril Formation of GroES and Determination of Cytotoxicity. Previously, we have studied the molecular mechanism underlying the formation of GroES protein fibrils from an unfolded state.[23−25] In order to investigate further the mechanism and consequences of GroES fibrillation, we carried out MTS assays[28,29] on Neuro-2a cells that were treated with samples of GroES obtained during the course of a typical fibrillation reaction. As shown in Figure 1A, the formation of fibrils by GroES may be traced through increases in ThioT fluorescence intensity. The results reflected a nucleus formation process (little or no fluorescence increase) during the first 48 h, followed by a rapid fluorescence increase that indicates fibril elongation, and the fluorescence attained a plateau after a 120 h incubation under the conditions we applied. In agreement with this basic time course, formation of aggregates and mature amyloid fibrils that were 14 ± 1.0 nm in width were observed by TEM as time progressed (Figure 2A−D). At appropriate times, soluble fractions and amyloid precipitate fractions were obtained, treated to remove Gdn-HCl, and added to samples to Neuro-2a culture. We observed that, while no impairment of cell function was detected upon addition of soluble GroES samples isolated at the zero time of the fibrillation reaction, the cell viability decreased significantly when samples of 48 h-incubated GroES were added (to 50% of the original viability). The toxicity of these detected intermediates (I48hr) was realized in a dose-dependent manner, and the IC50 of I48hr was determined to be 0.6 μM, as shown in Figure 1B. The I48hr samples were not fibrillar in form, as determined by TEM (Figure 2E), but rather granular in appearance, with diameters ranging from 44 to 88 nm. These forms were distinguishable from soluble protein images (Figure 2A). When soluble samples of GroES incubated for longer than 48 h were added to the cells, we observed a reversal of this effect, and no toxicity was observed when supernatants from mature amyloid fibrils were added (under our conditions, ∼10% of protein remained in the supernatant of mature fibril samples). In contrast to these results obtained strictly from soluble fractions, samples obtained from the pellet fractions did not affect cell viability, regardless of the incubation time.

We also evaluated the toxicity of various aggregate species of GroES formed separately from fibrillation to see if the toxicity observed in Figure 1A was specific only to the soluble samples of the fibril forming reaction obtained after 48 h (I48hr). We chose to fragment the mature fibrils samples using sonication for the experiments shown in Figure 1C, because the effective molar concentration of mature fibrils would be comparatively low if the protein concentration was used as a measure of normalization. The results in Figure 1C show that cell viability was indifferent to the addition of sonicated mature amyloid fibrils. Additionally, the cell viability was indifferent to the addition of various amorphous aggregate forms of GroES, which were collected from the supernatant and precipitate

dx.doi.org/10.1021/bi401135j | *Biochemistry* 2013, 52, 9202−9211

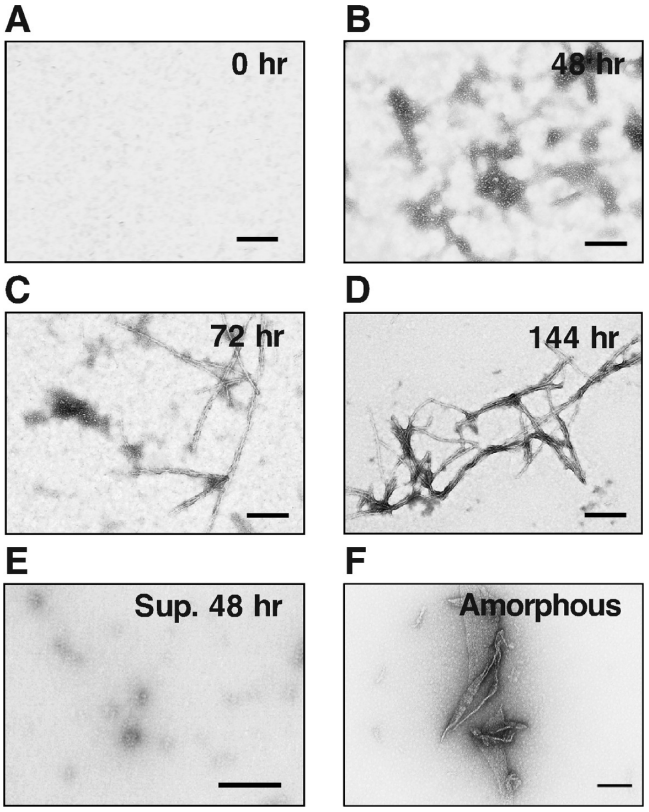

Figure 2. Differences in morphology of intermediate states formed during GroES fibrillation. TEM observation of the amyloid fibril formation process after the indicated incubation time (A–D), the toxic supernatant fraction obtained after a 48 h incubation (E), and acid-denatured amorphous species (F). The scale bar in each panel represents 200 nm.

fractions of GroES acid-denatured in glycine-HCl (pH 3.4), and 0.5 M Gdn-HCl (Figure 1D), respectively. The conditions where the amorphous aggregates were obtained (0.5 M Gdn-HCl and pH 3.4) correspond to conditions where the native GroES heptamer is in equilibrium with partially unfolded monomeric species.[19,24] TEM observation of these amorphous fractions showed that lamellar shape aggregates ranging from 30 to 900 nm in length were observable under these conditions (Figure 2F), and these forms were clearly different from rod-shaped fibrils. We also noted that the morphologies of the toxic aggregates differ from the amorphous aggregates. In order to further elucidate a general mechanism that explains the formation of toxic intermediate species of GroES protein during the course of fibril formation, we performed similar experiments using the GroES N51A mutant, whose fibrillation time course is slower compared to wild-type GroES.[25] As shown in Figure 1E, fibril formation of GroES N51A was detectable by fluorescence after incubation for 144 h and attained completion after an incubation time of 194 h. The process of fibril formation was clearly prolonged compared to the wild-type GroES protein. The cytotoxicity of GroES N51A fibril samples monitored by MTS assay indicated that cell toxicity was detectable in samples of GroEL N51A incubated for 144 h, whereas samples incubated for 194 h (matured fibrils) failed to display any cytotoxicity. The results show that cytotoxicity is attained only through intermediate aggregates of GroES that are soluble and formed specifically during the early stages of fibril assembly, rather than through mature amyloid fibrils or rapidly formed amorphous aggregates.

Next, to observe how the GroES aggregates specifically induce the disruption of neuronal cell function, we used an optical technique using $DiBAC_4(3)$, a voltage-sensitive membrane-resident bis-oxonol dye, which is capable of detecting immediate changes in membrane potential of cultured cells as an increase of fluorescence intensity.[30,31] The results of the $DiBAC_4(3)$ assay shown in Figure 3 demonstrate a

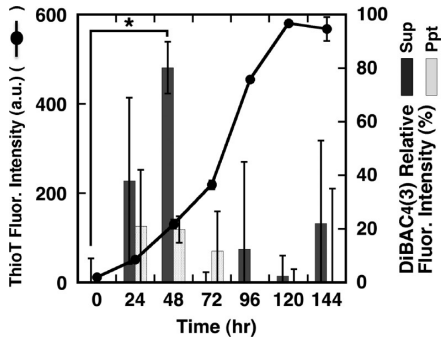

Figure 3. Effects of adding GroES samples obtained during amyloid fibril formation on cell membrane integrity. ThioT assay and $DiBAC_4(3)$ assay of incubated GroES. Aliquots of samples obtained at the indicated times were withdrawn and separated into the supernatant and precipitate fractions, followed by addition of each fraction to Neuro-2a cultures ($*p < 0.05$).

significant increase in the fluorescence intensity when cells were treated with cytotoxic I48hr samples of wild-type GroES, indicating that these aggregates invoked the depolarization of cell membrane. We therefore concluded that the soluble aggregates formed prior to mature amyloid fibrils interacted with the surface of cell membrane and disrupted its structural integrity, which subsequently induced cell death.

Inhibition of the Fibril Formation and Cytotoxicity by Polyphenols. We next attempted to examine if various polyphenols obtained from bilberry had any direct effects on GroES amyloid fibril formation. Bilberry is a rich source of natural polyphenols, and bilberry extracts are mainly composed of glycoside forms of various anthocyanins and a minor fraction of basic skeletal anthocyanidins that are detectable by HPLC and mass analysis.[32,33] Figure 4 shows the structures of delphinidin, cyanidin, del 3-gal, and cya 3-gal used in this study. These delphinidin-based and cyanidin-based polyphenols are relatively abundant in VMA. As shown in Figure 5A, when

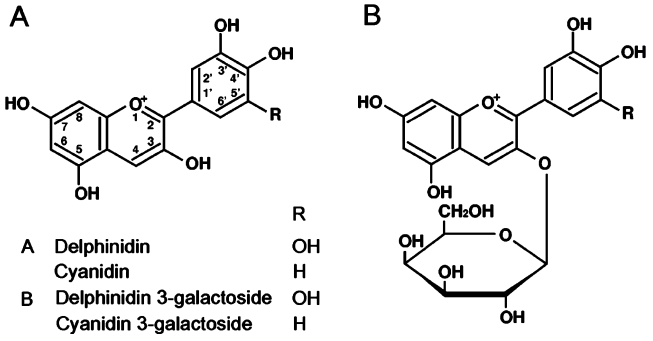

Figure 4. Chemical structures of (A) delphinidin, cyanidin, (B) del 3-gal, and cya 3-gal present in bilberry extracts.

dx.doi.org/10.1021/bi401135j | Biochemistry 2013, 52, 9202–9211

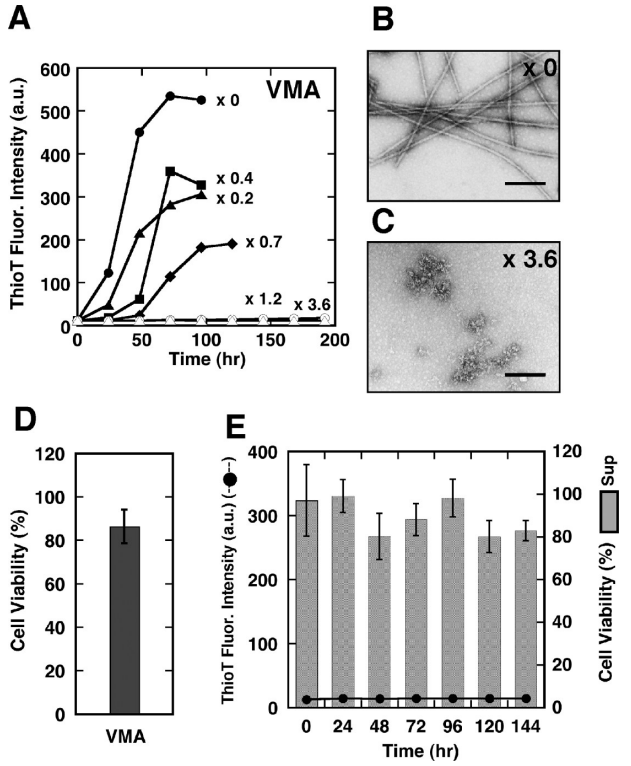

Figure 5. VMA prevents GroES fibril formation and the formation of toxic I48hr. (A) ThioT assay of GroES samples (96 μM) in the presence of VMA (0.2−3.6-fold molar ratio to GroES): Absence of VMA as control (circles), × 0.2 (triangles), × 0.4 (squares), × 0.7 (diamonds), × 1.2 (white circles), and × 3.6 VMA (white triangles). TEM observation of GroES samples formed in the absence (B) and the presence of 347 μM VMA (C). The scale bar in each panel represents 200 nm. (D) MTS assay of cells incubated with 347 μM VMA dissolved in 50 mM sodium phosphate buffer (pH 7.4). (E) MTS assay of cells in the presence of GroES sample supernatants obtained from aliquots of GroES incubated with 347 μM VMA for the indicated times. A trace of the ThioT fluorescence changes during incubation is also shown in the figure (closed circles).

VMA was added to GroES samples under conditions that promoted amyloid fibril formation, at concentrations corresponding to a 0.2−3.6-fold molar ratio to GroES, noticeable differences in the ThioT fluorescence intensity traces were observed. The increases in fluorescence that represented fibril formation of GroES were significantly suppressed in a VMA concentration-dependent manner up to 0.7-fold molar ratio and were completely inhibited in the presence of 1.2- and 3.6-fold VMA. In addition, the duration of the initial nucleus formation step was prolonged in the presence of VMA. TEM analysis revealed that, while mature amyloid fibrils of GroES were formed in the absence of VMA (Figure 5B), nonfibrillar and soluble aggregated species were formed in the presence of 3.6-fold VMA instead (Figure 5C). Detection of these soluble aggregated species raised an important question: whether these species formed in the presence of VMA were cytotoxic. To address this question, we conducted cell cytoxicity assays using these samples. It was observed that VMA, by itself, did not affect cell viability (Figure 5D). GroES samples incubated under fibril-promoting conditions with 3.6-fold VMA added remained soluble and were added to cell culture medium after the removal of Gdn-HCl following the procedure used in Figure 1A. Interestingly, no significant toxicity was detected for samples taken at any incubation time (Figure 5E). These data indicated that the polyphenols included in VMA were successful in inhibiting both the amyloid fibril formation of GroES and also the formation of toxic aggregated intermediates. From the presence of a new form of aggregate observed in Figure 5C in the presence of VMA, we deduced that GroES had been diverted from its initial fibril forming trajectory into a nontoxic aggregate form that represented an off-folding pathway.

We subsequently performed the fibril formation experiments in the presence of individually purified polyphenol components that are present in VMA. When we added 0.5- and 1.0-fold delphinidin to GroES fibrillation samples (Figure 6A), we observed prolonged nucleus formation times and a suppression of ThioT fluorescence increases that were analogous to the results shown in Figure 5. The increase in ThioT fluorescence was completely inhibited in the presence of higher concentrations of delphinidin (2-, 5-, 10-fold). TEM observation showed that nonfibrillar soluble aggregated species were formed in the presence of 10-fold delphinidin, which were distinct from the morphology seen in amyloid fibrils (Figure 6B−D). We carried out fibril formation experiments using various other polyphenols: cyanidin, del 3-gal, and cya 3-gal, the results of which are compared with those of delphinidin and VMA and plotted relative to the fluorescence intensities seen for the original GroES fibrillation reaction (Figure 6F). We found that cyanidin, del 3-gal, and cya 3-gal in particular effectively inhibited GroES amyloid fibril formation. Aggregates similar to those observed in samples containing delphinidin were observed in the presence of 10-fold del 3-gal (Figure 6E). Our results indicated that the effectiveness of fibril suppression decreased in the order VMA > anthocyanidins > anthocyanins. Considering the obtained data, the higher inhibitory effects of VMA might be attributed to a synergistic effect of various polyphenols included in VMA. From these experiments, it was demonstrated that the inhibitory effects of VMA on the amyloid fibril formation of GroES could be attributed to each individual polyphenol present in VMA. Notably, our results also suggested the importance of the anthocyanidin moiety, rather than the sugar moiety.

Dissolution of the Fibrils and Neutralization of Cytotoxicity by VMA. Since the experiments in Figure 6 demonstrated that polyphenols in VMA were capable of suppressing the formation of GroES fibrils, we were curious to determine if VMA could affect the characteristics of preformed aggregate forms of GroES. Accordingly, we performed a delayed-addition assay of VMA into samples of wild-type GroES undergoing fibrillation. Very surprisingly, as shown in Figure 7A, addition of 3.6-fold VMA at 48, 96, and 120 h of the fibrillation reaction all resulted in a decrease in the ThioT fluorescence intensities. Typical amyloid fibrils of GroES formed after a 120 h incubation as observed by AFM (Figure 7B) were almost completely dissolved when incubated for 48 h with VMA (Figure 7C, sample corresponds to Figure 7A, red, 168 h). As shown in Figure 7D, the toxicity of the I48hr intermediate species was also neutralized; that is, by adding 3.6-fold VMA into the I48hr samples and incubating for 3 h, cytotoxicity of these samples were almost completely suppressed (as seen by the increase in cell viability from 35% to 93% for VMA treated I48hr samples, Figure 7D). Analogous results were also obtained in $DiBAC_4(3)$ assays. We also determined during this assay that VMA in fact prevented the initial formation of cytotoxic GroES aggregates when the

dx.doi.org/10.1021/bi401135j | *Biochemistry* 2013, 52, 9202−9211

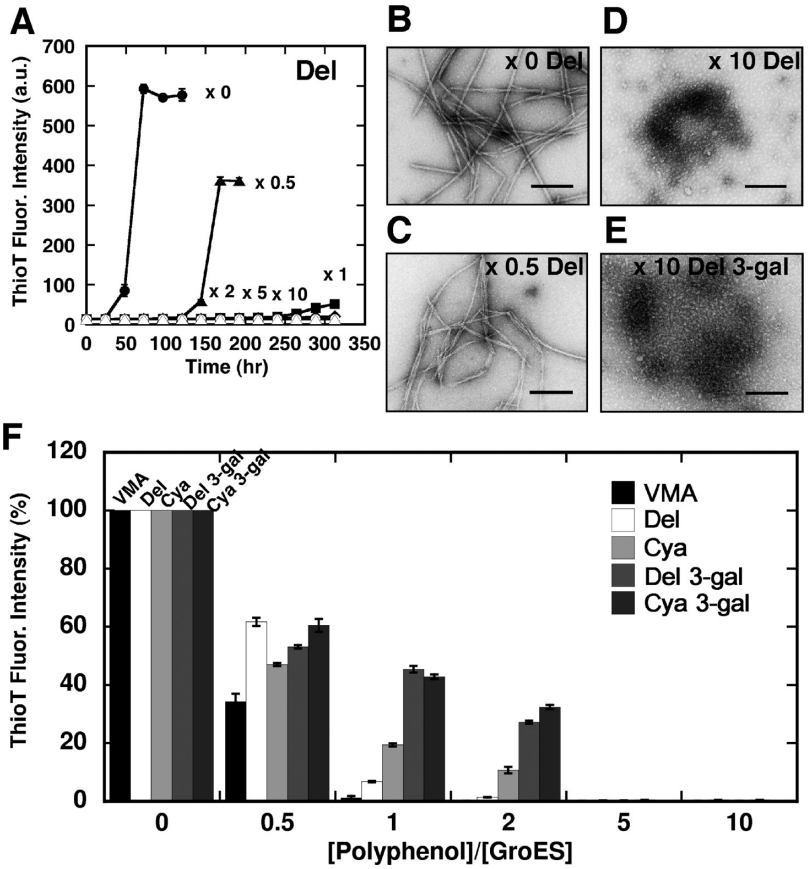

Figure 6. Inhibition of GroES fibril formation by pure polyphenols. (A) Fibril formation experiments of GroES in the presence of delphinidin (0.5–10-fold molar ratio): Absence of delphinidin as control (circles), × 0.5 (triangles), × 1 (squares), × 2 (diamonds), × 5 (white circles), and × 10 delphinidin (white triangles). TEM images after incubation in the absence (B), and the presence of 0.5-fold (C), and 10-fold delphinidin (D), as well as in the presence of 10-fold del 3-gal (E). The scale bar in each panel represents 200 nm. (F) ThioT assays in the presence of VMA, delphinidin, cyanidin, del 3-gal, and cya 3-gal. The ThioT fluorescence intensities in the absence of polyphenols after incubation was set to 100%, and those in the presence of polyphenols were plotted in each concentrations as [polyphenol]/[GroES].

polyphenols were added prior to the beginning of the fibrillation reaction.

In order to understand how polyphenol inhibits fibril formation and/or dissolves the cytotoxic intermediates, we attempted to detect the interactions between VMA polyphenols and GroES protein. After incubation of unfolded GroES protein for 48 h in the presence of 3.6-fold VMA, under which conditions the toxic soluble intermediates were not produced, we measured the absorption spectra of desalted sample, reasoning that if VMA polyphenol binds to GroES protein, it should be detectable by absorption measurement after this treatment. As shown in Figure 7E, the desalted sample showed an increase in absorbance within a broad absorbance range from 350 nm to 600 nm. This wavelength region corresponds to a region where anthocyanins strongly absorb light;[34] however, a lack of distinct absorbance peaks might suggest that this increase in absorbance was caused by light scattering from aggregated GroES. However, when we monitored the absorbance spectra of VMA over a 24 h interval (Figure 7E, inset), we found that the absorption spectra of VMA gradually changed during this time. This phenomenon has been correlated with oxidation of the polyphenols in VMA after prolonged incubation.[35,36] When we compared the spectra of the desalted GroES-VMA incubated sample with the absorbance spectra of pure VMA incubated for 24 h, we now observed that the two spectra closely matched (Figure 7E, compare red and black traces of the main panel). This suggests that VMA bound tightly to GroES during the fibrillation reaction and thereby suppressed and dissolved aggregated GroES species. We note here that samples of I48hr incubated with VMA for 24 h also showed a similar absorbance spectrum (data not shown). These findings demonstrate that VMA polyphenol actively interacts with GroES protein molecules in the unfolded, solubly aggregated, and fibrillated forms. This polyphenol bound form of GroES protein was most likely rerouted to form soluble or nontoxic alternate aggregates (Figures 5C and 6E).

■ DISCUSSION

Cytotoxicity of Intermediate Species Formed from Disease-Unrelated Proteins; Implication of General Property of Fibril Formation and Toxicity in Proteins. The causative relationship between several neurodegenerative diseases and the formation of amyloid-like fibrils by various intrinsically disordered proteins[1,4,5] is a scientific puzzle that, when solved, will provide many medical and societal benefits. Studies to date indicate that amyloid oligomers, rather than mature fibrils, play important roles of the impairment of cell viability.[8,9] It has also been reported that proteins, such as the SH3 domain of bovine phosphatidyl-inositol-3′-kinase (PI3-SH3) and the N-terminal domain of the *E. coli* HypF protein (HypF-N), proteins that are not directly implicated in diseases,

dx.doi.org/10.1021/bi401135j | *Biochemistry* 2013, 52, 9202–9211

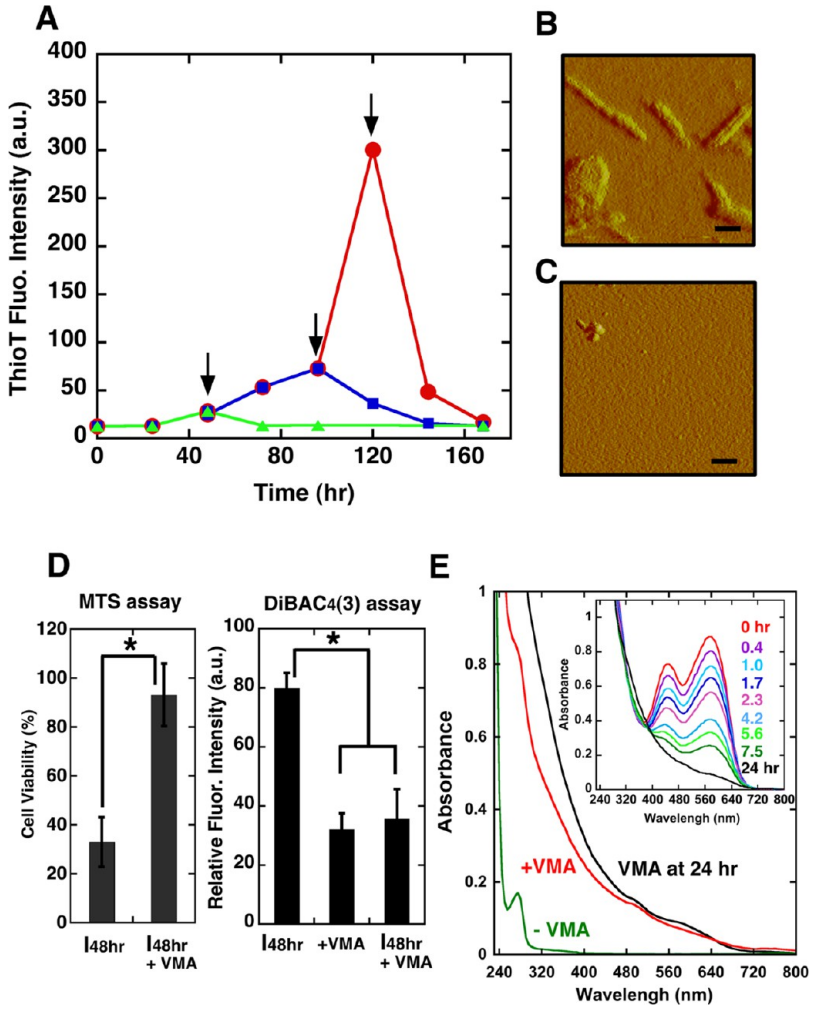

Figure 7. VMA is able to dissolve preformed I48hr intermediates and mature fibrils of GroES and neutralize cytotoxicity. (A) Delayed addition of 3.6-fold VMA to GroES samples incubated for 48 (green triangles), 96 (blue squares), and 120 h (red circles) under conditions promoting fibril formation. VMA addition times are denoted by an arrow in each sample. (B) AFM image of GroES amyloid fibrils obtained after a 120 h incubation (120hr after the start of the experiment, panel A, red, arrow). (C) Typical AFM image obtained after VMA was added to samples shown in panel B and subsequently incubated for 48 h (168 h after the start of the experiment, panel A, red). The scale bar in each panel represents 200 nm. (D) MTS assay (cell viability) and $DiBAC_4(3)$ assay (membrane potential) of cells incubated with GroES I48hr samples and preformed I48hr incubated with VMA. VMA (3.6-fold) was added to I48hr samples (denoted by I48hr + VMA), and the assay was performed after 3 h incubation at 25 °C (*p < 0.05). In the $DiBAC_4(3)$ assays, the sample denoted +VMA indicates results of an assay performed by adding GroES fibrillation samples formed in the presence of VMA. (E) Absorption spectra analysis to detect polyphenols bound to GroES protein. +VMA; typical absorption spectrum of GroES fibrillation samples formed in the presence of 3.6-fold VMA. Inset figure shows absorption spectra of VMA dissolved in fibril formation buffer measured after an incubation at 25 °C for the indicated times. The 24 h trace is reproduced in the main panel (in black) for comparison.

form fibrils *in vitro* that closely resemble the specific molecular forms associated with neurodegenerative disorders.[10,37] The cytotoxicity of the protein deposits was, in both of these cases, found in the initial, rapidly formed nonfibrillar aggregates rather than the highly organized fibrillar structures.[11] Cytotoxicity for PI3-SH3 was observed in rapidly formed granular aggregates with a diameter ranging between 4−200 nm. In the case of HypF-N protein, nonfibrillar and nongranular aggregates, and some aggregates resembling protofibrils were shown to be highly toxic. These data indicate that the ability of certain protein aggregates, that subsequently form amyloid fibrils, to impair cell viability might be a common phenomenon, not simply limited to proteins that have already been implicated in various diseases.[11,38−41] It has been proposed that the ability to form amyloid fibrils and toxic structures may be itself a general property of proteins.[10,11,41−43]

Here, toxicity assays for mouse Neuro-2a cells were performed using various aggregates of GroES, as shown in Figure 1−3. From the MTS assays shown in Figure 1, we found that soluble intermediate aggregates that were formed during fibril formation process displayed toxicity toward neuronal cell cultures, but intact mature fibrils, sonicated mature fibrils, and amorphous aggregates did not. The toxic intermediate aggregates were nonfibrillar, as seen in Figure 2E, and were formed during the early stages of the amyloid fibril formation reaction. The results from $DiBAC_4(3)$ assays shown in Figure 3 suggested that these aggregates would interact with the surface of cell membrane and perturb the membrane potential, as observed by the specific increase of fluorescence intensities. We also attempted to determine the localization of I48hr in the cell when it displays cytotoxicity and found that I48hr (GroES protein) was detected mainly in the soluble cytoplasmic fractions of Neuro-2a cell extracts, and almost none in

dx.doi.org/10.1021/bi401135j | *Biochemistry* 2013, 52, 9202−9211

detergent-solubilized membrane fractions, as determined by SDS-PAGE analysis (data not shown). The mechanism of I48hr permeation may involve hydrophobic surfaces that are exposed in the early aggregates that are more accessible to nonspecifically interact with cell membrane compared to the corresponding regions in mature fibrils.[11,40,44,45] Fully formed fibrils, in fact, are characterized by a trait which is qualitatively opposite to the notion raised here; fibrils typically possess a protease-resistant, solvent-inaccessible sequence region thought to represent the fiber core.[24,27] These results suggest the importance of elucidating the inherent structural properties of various aggregated protein forms.

Bilberry Polyphenols Contain Powerful Inhibitory Agents That Are Capable of Altering the Fibril Formation Reaction and Also Have the Ability To Dissolve Amyloid Fibrils and Neutralize Cytotoxic Species. One important strategy for inhibiting amyloid fibril formation and associated cytotoxicity involves the use of small molecular compounds that directly interact with amyloidogenic proteins.[12] Polyphenols that are abundant in bilberries have structures similar to the polyphenol inhibitors,[12,13] as exemplified by green tea polyphenol (−)-epigallocatechin-3-gallate (EGCG) which acts as an inhibitory agent for *in vitro* amyloid fibril formation of intrinsically disordered proteins such as Aβ, α-synuclein, huntingtin, and the model polypeptide κ-casein.[46−48] We performed amyloid fibril formation experiments in the presence of VMA and pure polyphenols present in VMA: anthocyanidins and anthocyanins. Anthocyanidins strongly inhibited GroES fibril formation, and anthocyanins that are abundantly included in bilberry also showed inhibitory effects, indicating the importance of the anthocyanidin skeleton (Figure 6). From absorption measurement analysis (Figure 7E), we found that VMA polyphenols bound strongly to GroES. However, when we performed NMR measurements (^{1}H−^{15}N HSQC) of GroES samples in the presence of Gdn-HCl and cyanidin, reliable data could not be obtained, perhaps because the effect of Gdn-HCl as a strong chaotropic agent was dominant in the time scale of NMR measurements compared to the interactions between GroES and cyanidin (data not shown).

The most striking finding was the dissolving effect of VMA toward protein aggregates including amyloid fibrils of GroES (Figure 7A−C). Addition of VMA into samples containing toxic intermediates (I48hr) neutralized their toxicity (Figure 7D). This neutralization was explained simply by the ability of VMA to dissolve I48hr (Figure 7C). Although VMA polyphenol binding to GroES protein was detected (Figure 7E), details of this binding remain to be elucidated, for example, the specific structural derivative of VMA that actually binds to GroES, as well as determining the binding mechanism (specific site(s)? covalent or noncovalent binding?). These issues will be addressed in a separate study.

The aggregated species that were formed in the presence of bilberry polyphenols and remained soluble were not toxic to neuronal cells (Figure 5). It is reported that catechin and epicatechin were absorbed after oral administration to rats and present in plasma as intact and metabolites forms including 3′-*O*-methylated and 5-*O*-β-glucuronide-conjugated forms.[49] Additionally, epicatechin glucuronide and 3′-*O*-methyl epicatechin glucuronide were detected after oral ingestion in rat brain tissues.[50] Anthocyanins were rapidly absorbed as glycosides in rats and human, and the intact glycosidic forms were detected in plasma after oral administration.[51−55] Experiments showed that the anthocyanins were able to cross the blood-brain barrier in rats fed with supplemented anthocyanin mixtures for 15 days,[56] as well as after a single administration.[57] Intact delphinidin 3-galactoside and cyanidin 3-galactoside were also observed in the brain of pigs which were a suitable model for human digestive absorption,[58] indicating that anthocyanins can have a direct effect on brain processes.[59]

All of these results demonstrate that polyphenols possess the ability to permeate into regions that are important in a variety of neurological disorders and therefore imply that a treatment based upon the action of these polyphenols on intrinsically disordered proteins that cause neurodegenerative diseases is feasible. In this context, studies regarding α-synuclein, an intrinsically disordered protein implicated in Parkinson's disease in its fibrillation, are ongoing.

■ CONCLUSIONS

In the present study, we determined that aggregates of co-chaperonin GroES formed during the course of amyloid fibril formation were toxic to neuronal cells, and polyphenols included in bilberry were capable of inhibiting toxic intermediate and fibril formation, as well as dissolving preformed toxic aggregates and mature fibrils. The former result raises the possibility that small amounts of intracellular proteins that are not clearly implicated in disease development may spontaneously assemble into aggregates and impair cellular function. And the latter results point toward a role for bilberry polyphenols in controlling the fibril formation of various proteins related to neurodegenerative diseases and development of a therapeutic reagent. Understanding the molecular interactions between small molecules and specific regions of amyloidogenic proteins also would lead to the elucidation of a general mechanism of amyloid fibril formation. For both pathogenic and nonpathogenic proteins, studies to clarify the relationship between fibril formation and cytotoxicity of early stage aggregates, as well as their control, are of crucial importance in the prevention and treatment of neurodegenerative diseases.

■ AUTHOR INFORMATION

Corresponding Author

*Tel/Fax: +81-857-31-5271. E-mail: kawata@bio.tottori-u.ac.jp.

Author Contributions

#These authors contributed equally to this work.

Funding

This work was supported in part by grants-in-aid for Scientific Research from the Japan Society for the Promotion of Science (JSPS) and the Ministry of Education, Culture, Sports, Science, and Technology of Japan, and the X-ray Free Electron Laser Priority Strategy Program (MEXT). Portions of this study have also been supported by financial aid from Wakasa Seikatsu, Co, Japan.

Notes

The authors declare the following competing financial interest(s): Potential Conflicts of Interest: This study was performed in cooperation with Wakasa Seikatsu, Co. Japan, which markets bilberry extracts commercially to the domestic market in Japan as a dietary supplement. One of the coauthors (SK) is an employee of Wakasa Seikatsu, Co. Samples of bilberry extracts used in this study were provided by Wakasa Seikatsu, Co. These affiliations affect none of the following

components of this study: the experimental design, the experimental process, the interpretation of experimental results, and subsequent sharing and disclosure of scientific materials to the community.

■ ACKNOWLEDGMENTS

We thank Ms. E. Kawahara and Ms. Miho Taniguchi of Tottori University for technical assistance in measurements of electron microscopy.

■ ABBREVIATIONS

cya 3-gal, cyanidin 3-galactoside; del 3-gal, delphinidin 3-galactoside; $DiBAC_4(3)$, bis-(1,3-dibutylbarbituric acid) trimethine oxonol; Gdn-HCl, guanidine hydrochloride; TEM, transmission electron microscopy; VMA, extracts of bilberry (*Vaccinium myrtillus* anthocyanoside)

■ REFERENCES

(1) Selkoe, D. J. (2003) Folding proteins in fatal ways. *Nature 426*, 900−904.
(2) Makin, O. S., and Serpell, L. C. (2002) Examining the structure of the mature amyloid fibril. *Biochem. Soc. Trans. 30*, 521−525.
(3) Ohnishi, S., and Takano, K. (2004) Amyloid fibrils from the viewpoint of protein folding. *Cell. Mol. Life Sci. 61*, 511−524.
(4) Uversky, V. N., Oldfield, C. J., Midic, U., Xie, H. B., Xue, B., Vucetic, S., Iakoucheva, L. M., Obradovic, Z., and Dunker, A. K. (2009) Unfoldomics of human diseases: linking protein intrinsic disorder with diseases. *BMC Genomics 10* (Suppl. 1), No. S7.
(5) Uversky, V. N. (2008) Amyloidogenesis of natively unfolded proteins. *Curr. Alzheimer Res. 5*, 260−287.
(6) Wright, P. E., and Dyson, H. J. (1999) Intrinsically unstructured proteins: re-assessing the protein structure-function paradigm. *J. Mol. Biol. 293*, 321−331.
(7) Fink, A. L. (2005) Natively unfolded proteins. *Curr. Opin. Struct. Biol. 15*, 35−41.
(8) Kitamura, A., and Kubota, H. (2010) Amyloid oligomers: dynamics and toxicity in the cytosol and nucleus. *FEBS J. 277*, 1369−1379.
(9) Karpinar, D. P., Balija, M. B., Kugler, S., Opazo, F., Rezaei-Ghaleh, N., Wender, N., Kim, H. Y., Taschenberger, G., Falkenburger, B. H., Heise, H., Kumar, A., Riedel, D., Fichtner, L., Voigt, A., Braus, G. H., Giller, K., Becker, S., Herzig, A., Baldus, M., Jackle, H., Eimer, S., Schulz, J. B., Griesinger, C., and Zweckstetter, M. (2009) Pre-fibrillar alpha-synuclein variants with impaired beta-structure increase neurotoxicity in Parkinson's disease models. *EMBO J. 28*, 3256−3268.
(10) Guijarro, J. I., Sunde, M., Jones, J. A., Campbell, I. D., and Dobson, C. M. (1998) Amyloid fibril formation by an SH3 domain. *Proc. Natl. Acad. Sci. U. S. A. 95*, 4224−4228.
(11) Bucciantini, M., Giannoni, E., Chiti, F., Baroni, F., Formigli, L., Zurdo, J., Taddei, N., Ramponi, G., Dobson, C. M., and Stefani, M. (2002) Inherent toxicity of aggregates implies a common mechanism for protein misfolding diseases. *Nature 416*, 507−511.
(12) Porat, Y., Abramowitz, A., and Gazit, E. (2006) Inhibition of amyloid fibril formation by polyphenols: structural similarity and aromatic interactions as a common inhibition mechanism. *Chem. Biol. Drug Des. 67*, 27−37.
(13) Masuda, M., Suzuki, N., Taniguchi, S., Oikawa, T., Nonaka, T., Iwatsubo, T., Hisanaga, S., Goedert, M., and Hasegawa, M. (2006) Small molecule inhibitors of alpha-synuclein filament assembly. *Biochemistry 45*, 6085−6094.
(14) Bukau, B., and Horwich, A. L. (1998) The Hsp70 and Hsp60 chaperone machines. *Cell 92*, 351−366.
(15) Hartl, F. U., and Hayer-Hartl, M. (2002) Molecular chaperones in the cytosol: from nascent chain to folded protein. *Science 295*, 1852−1858.
(16) Xu, Z., Horwich, A. L., and Sigler, P. B. (1997) The crystal structure of the asymmetric GroEL-GroES-(ADP)7 chaperonin complex. *Nature 388*, 741−750.
(17) Hunt, J. F., Weaver, A. J., Landry, S. J., Gierasch, L., and Deisenhofer, J. (1996) The crystal structure of the GroES co-chaperonin at 2.8 A resolution. *Nature 379*, 37−45.
(18) Seale, J. W., Gorovits, B. M., Ybarra, J., and Horowitz, P. M. (1996) Reversible oligomerization and denaturation of the chaperonin GroES. *Biochemistry 35*, 4079−4083.
(19) Higurashi, T., Nosaka, K., Mizobata, T., Nagai, J., and Kawata, Y. (1999) Unfolding and refolding of Escherichia coli chaperonin GroES is expressed by a three-state model. *J. Mol. Biol. 291*, 703−713.
(20) Higurashi, T., Hiragi, Y., Ichimura, K., Seki, Y., Soda, K., Mizobata, T., and Kawata, Y. (2003) Structural stability and solution structure of chaperonin GroES heptamer studied by synchrotron small-angle X-ray scattering. *J. Mol. Biol. 333*, 605−620.
(21) Boudker, O., Todd, M. J., and Freire, E. (1997) The structural stability of the co-chaperonin GroES. *J. Mol. Biol. 272*, 770−779.
(22) Panda, M., Ybarra, J., and Horowitz, P. M. (2001) High hydrostatic pressure can probe the effects of functionally related ligands on the quaternary structures of the chaperonins GroEL and GroES. *J. Biol. Chem. 276*, 6253−6259.
(23) Higurashi, T., Yagi, H., Mizobata, T., and Kawata, Y. (2005) Amyloid-like fibril formation of co-chaperonin GroES: nucleation and extension prefer different degrees of molecular compactness. *J. Mol. Biol. 351*, 1057−1069.
(24) Yagi, H., Sato, A., Yoshida, A., Hattori, Y., Hara, M., Shimamura, J., Sakane, I., Hongo, K., Mizobata, T., and Kawata, Y. (2008) Fibril formation of hsp10 homologue proteins and determination of fibril core regions: differences in fibril core regions dependent on subtle differences in amino acid sequence. *J. Mol. Biol. 377*, 1593−1606.
(25) Iwasa, H., Meshitsuka, S., Hongo, K., Mizobata, T., and Kawata, Y. (2011) Covalent structural changes in unfolded GroES that lead to amyloid fibril formation detected by NMR: Insight into intrinsically disordered proteins. *J. Biol. Chem. 286*, 21796−21805.
(26) Makio, T., Arai, M., and Kuwajima, K. (1999) Chaperonin-affected refolding of alpha-lactalbumin: effects of nucleotides and the co-chaperonin GroES. *J. Mol. Biol. 293*, 125−137.
(27) Yagi, H., Takeuchi, H., Ogawa, S., Ito, N., Sakane, I., Hongo, K., Mizobata, T., Goto, Y., and Kawata, Y. (2010) Isolation of short peptide fragments from alpha-synuclein fibril core identifies a residue important for fibril nucleation: a possible implication for diagnostic applications. *Biochim. Biophys. Acta 1804*, 2077−2087.
(28) Lasagna-Reeves, C. A., Castillo-Carranza, D. L., Guerrero-Muoz, M. J., Jackson, G. R., and Kayed, R. (2010) Preparation and characterization of neurotoxic tau oligomers. *Biochemistry 49*, 10039−10041.
(29) Barltrop, J. A., Owen, T. C., Cory, A. H., and Cory, J. G. (1991) 5-(3-Carboxymethoxyphenyl)-2-(4,5-dimethylthiazolyl)-3-(4-sulfophenyl)tetrazolium, Inner Salt (Mts) and Related Analogs of 3-(4,5-Dimethylthiazolyl)-2,5-diphenyltetrazolium Bromide (Mtt) Reducing to Purple Water-Soluble Formazans as Cell-Viability Indicators. *Bioorg. Med. Chem. Lett. 1*, 611−614.
(30) Epps, D. E., Wolfe, M. L., and Groppi, V. (1994) Characterization of the Steady-State and Dynamic Fluorescence Properties of the Potential-Sensitive Dye Bis-(1,3-Dibutylbarbituric acid)trimethine Oxonol (Dibac(4)(3)) in Model Systems and Cells. *Chem. Phys. Lipids 69*, 137−150.
(31) Blanchard, B. J., Thomas, V. L., and Ingram, V. M. (2002) Mechanism of membrane depolarization caused by the Alzheimer Abeta1−42 peptide. *Biochem. Biophys. Res. Commun. 293*, 1197−1203.
(32) Ishikawa, F., Oishi, M., Shindo, T., Horie, M., Yasui, A., and Nakazato, M. (2008) Analysis of Anthocyanins in Dietary Supplements Containing Blueberry Extract. *J. Food Hyg. Soc. Jpn. 49*, 339−346.
(33) Ichiyanagi, T., Hatano, Y., Matsugo, S., and Konishi, T. (2004) Structural dependence of HPLC separation pattern of Anthocyanins from bilberry (Vaccinium myrtillus L.). *Chem. Pharm. Bull. 52*, 628−630.

(34) Burdulis, D., Ivanauskas, L., Dirse, V., Kazlauskas, S., and Razukas, A. (2007) Study of diversity of anthocyanin composition in bilberry (Vaccinium myrtillus L.) fruits. *Medicina (Kaunas) 43*, 971−977.
(35) Osmani, S. A., Hansen, E. H., Malien-Aubert, C., Olsen, C. E., Bak, S., and Moller, B. L. (2009) Effect of glucuronosylation on anthocyanin color stability. *J. Agric. Food Chem. 57*, 3149−3155.
(36) Meng, X., Munishkina, L. A., Fink, A. L., and Uversky, V. N. (2009) Molecular mechanisms underlying the flavonoid-induced inhibition of alpha-synuclein fibrillation. *Biochemistry 48*, 8206−8224.
(37) Chiti, F., Bucciantini, M., Capanni, C., Taddei, N., Dobson, C. M., and Stefani, M. (2001) Solution conditions can promote formation of either amyloid protofilaments or mature fibrils from the HypF N-terminal domain. *Protein Sci. 10*, 2541−2547.
(38) Conway, K. A., Lee, S. J., Rochet, J. C., Ding, T. T., Williamson, R. E., and Lansbury, P. T. (2000) Acceleration of oligomerization, not fibrillization, is a shared property of both alpha-synuclein mutations linked to early-onset Parkinson's disease: Implications for pathogenesis and therapy. *Proc. Natl. Acad. Sci. U. S. A. 97*, 571−576.
(39) Lambert, M. P., Barlow, A. K., Chromy, B. A., Edwards, C., Freed, R., Liosatos, M., Morgan, T. E., Rozovsky, I., Trommer, B., Viola, K. L., Wals, P., Zhang, C., Finch, C. E., Krafft, G. A., and Klein, W. L. (1998) Diffusible, nonfibrillar ligands derived from Abeta1−42 are potent central nervous system neurotoxins. *Proc. Natl. Acad. Sci. U. S. A. 95*, 6448−6453.
(40) Stefani, M. (2010) Biochemical and biophysical features of both oligomer/fibril and cell membrane in amyloid cytotoxicity. *FEBS J. 277*, 4602−4613.
(41) Stefani, M., and Dobson, C. M. (2003) Protein aggregation and aggregate toxicity: new insights into protein folding, misfolding diseases and biological evolution. *J. Mol. Med. 81*, 678−699.
(42) Chiti, F., Webster, P., Taddei, N., Clark, A., Stefani, M., Ramponi, G., and Dobson, C. M. (1999) Designing conditions for in vitro formation of amyloid protofilaments and fibrils. *Proc. Natl. Acad. Sci. U. S. A. 96*, 3590−3594.
(43) Bucciantini, M., Calloni, G., Chiti, F., Formigli, L., Nosi, D., Dobson, C. M., and Stefani, M. (2004) Prefibrillar amyloid protein aggregates share common features of cytotoxicity. *J. Biol. Chem. 279*, 31374−31382.
(44) Cheon, M., Chang, I., Mohanty, S., Luheshi, L. M., Dobson, C. M., Vendruscolo, M., and Favrin, G. (2007) Structural reorganisation and potential toxicity of oligomeric species formed during the assembly of amyloid fibrils. *PLoS Comput. Biol. 3*, 1727−1738.
(45) Bolognesi, B., Kumita, J. R., Barros, T. P., Esbjorner, E. K., Luheshi, L. M., Crowther, D. C., Wilson, M. R., Dobson, C. M., Favrin, G., and Yerbury, J. J. (2010) ANS binding reveals common features of cytotoxic amyloid species. *ACS Chem. Biol. 5*, 735−740.
(46) Ehrnhoefer, D. E., Bieschke, J., Boeddrich, A., Herbst, M., Masino, L., Lurz, R., Engemann, S., Pastore, A., and Wanker, E. E. (2008) EGCG redirects amyloidogenic polypeptides into unstructured, off-pathway oligomers. *Nat. Struct. Mol. Biol. 15*, 558−566.
(47) Ehrnhoefer, D. E., Duennwald, M., Markovic, P., Wacker, J. L., Engemann, S., Roark, M., Legleiter, J., Marsh, J. L., Thompson, L. M., Lindquist, S., Muchowski, P. J., and Wanker, E. E. (2006) Green tea (−)-epigallocatechin-gallate modulates early events in huntingtin misfolding and reduces toxicity in Huntington's disease models. *Hum. Mol. Genet. 15*, 2743−2751.
(48) Hudson, S. A., Ecroyd, H., Dehle, F. C., Musgrave, I. F., and Carver, J. A. (2009) (−)-epigallocatechin-3-gallate (EGCG) maintains kappa-casein in its pre-fibrillar state without redirecting its aggregation pathway. *J. Mol. Biol. 392*, 689−700.
(49) Baba, S., Osakabe, N., Natsume, M., Muto, Y., Takizawa, T., and Terao, J. (2001) In vivo comparison of the bioavailability of (+)-catechin, (-)-epicatechin and their mixture in orally administered rats. *J. Nutr. 131*, 2885−2891.
(50) Abd El Mohsen, M. M., Kuhnle, G., Rechner, A. R., Schroeter, H., Rose, S., Jenner, P., and Rice-Evans, C. A. (2002) Uptake and metabolism of epicatechin and its access to the brain after oral ingestion. *Free Radical Bio. Med. 33*, 1693−1702.
(51) Tsuda, T., Horio, F., and Osawa, T. (1999) Absorption and metabolism of cyanidin 3-*O*-beta-D-glucoside in rats. *FEBS Lett. 449*, 179−182.
(52) Miyazawa, T., Nakagawa, K., Kudo, M., Muraishi, K., and Someya, K. (1999) Direct intestinal absorption of red fruit anthocyanins, cyanidin-3-glucoside and cyanidin-3,5-diglucoside, into rats and humans. *J. Agric. Food Chem. 47*, 1083−1091.
(53) Matsumoto, H., Inaba, H., Kishi, M., Tominaga, S., Hirayama, M., and Tsuda, T. (2001) Orally administered delphinidin 3-rutinoside and cyanidin 3-rutinoside are directly absorbed in rats and humans and appear in the blood as the intact forms. *J. Agric. Food Chem. 49*, 1546−1551.
(54) Cao, G., Muccitelli, H. U., Sanchez-Moreno, C., and Prior, R. L. (2001) Anthocyanins are absorbed in glycated forms in elderly women: a pharmacokinetic study. *Am. J. Clin. Nutr. 73*, 920−926.
(55) Felgines, C., Texier, O., Besson, C., Fraisse, D., Lamaison, J. L., and Remesy, C. (2002) Blackberry anthocyanins are slightly bioavailable in rats. *J. Nutr. 132*, 1249−1253.
(56) Talavera, S., Felgines, C., Texier, O., Besson, C., Gil-Izquierdo, A., Lamaison, J. L., and Remesy, C. (2005) Anthocyanin metabolism in rats and their distribution to digestive area, kidney, and brain. *J. Agric. Food Chem. 53*, 3902−3908.
(57) Passamonti, S., Vrhovsek, U., Vanzo, A., and Mattivi, F. (2005) Fast access of some grape pigments to the brain. *J. Agric. Food Chem. 53*, 7029−7034.
(58) Kalt, W., Blumberg, J. B., McDonald, J. E., Vinqvist-Tymchuk, M. R., Fillmore, S. A., Graf, B. A., O'Leary, J. M., and Milbury, P. E. (2008) Identification of anthocyanins in the liver, eye, and brain of blueberry-fed pigs. *J. Agric. Food Chem. 56*, 705−712.
(59) Barros, D., Amaral, O. B., Izquierdo, I., Geracitano, L., do Carmo Bassols Raseira, M., Henriques, A. T., and Ramirez, M. R. (2006) Behavioral and genoprotective effects of Vaccinium berries intake in mice. *Pharmacol., Biochem. Behav. 84*, 229−234.